

# High-resolution modelling of mid-Holocene New Zealand climate at 6000 yr BP

The Holocene  
23(9) 1272–1285  
© The Author(s) 2013  
Reprints and permissions:  
sagepub.co.uk/journalsPermissions.nav  
DOI: 10.1177/0959683613484612  
hol.sagepub.com  


Duncan Ackerley,<sup>1,8</sup> Andrew Lorrey,<sup>2</sup> James Renwick,<sup>3</sup>  
Steven J Phipps,<sup>4,5</sup> Sebastian Wagner<sup>6</sup> and Anthony Fowler<sup>7</sup>

## Abstract

Palaeoclimate-proxy data provide an invaluable source of evidence for past climatic conditions, which can be compared with data from climate model simulations. This study illustrates how high-resolution regional climate model simulations can be used to estimate the difference in the climate of New Zealand between 6000 years before present (yr BP) and the pre-industrial era (c. AD 1750). Four pairs (pre-industrial and 6000 yr BP) of atmosphere-only global and regional climate model simulations were run with prescribed sea surface temperatures (SST). The SSTs are derived from four different fully coupled ocean–atmosphere general circulation model simulations, resulting in a different lower-boundary forcing in each of the atmosphere-only simulations. We find evidence for generally cooler conditions and for wetter (drier) conditions over eastern (western) New Zealand 6000 yr BP. The work compares well with model and proxy estimates of temperature and precipitation in the New Zealand region between 7000 and 6000 yr BP. The results also highlight the added value of regional model studies in regions with such complex terrain as New Zealand. This study also shows the limitations of applying uniformitarian principles when downscaling global model fields (and ‘up-scaling’ palaeo-proxy data) to infer past climatic conditions.

## Keywords

circulation, mid-Holocene climate, New Zealand, palaeoclimate, PMIP2, precipitation, sea level pressure, regional climate model, temperature

Received 13 April 2012; revised manuscript accepted 1 March 2013

## Introduction

The Holocene is a geological epoch that encompasses the last 12,000 years. The mid Holocene roughly corresponds to 6000 years before present (yr BP) and is a time when Earth’s orbital parameters (eccentricity, obliquity and angular precession, see Braconnot et al., 2007a) were different to the present day, particularly the angular precession. Consequently, at 6000 yr BP, seasonal incoming solar radiation (insolation) at the top of the Earth’s atmosphere (and subsequently at the surface too) was also different to the present day. Changes in insolation have been shown in previous modelling studies to have an impact on the surface climate (see Braconnot et al., 2007a, 2007b). These impacts can also be seen in the proxy data evidence (for example see Zhang et al., 2010, which includes a model/proxy data comparison for Northern Hemisphere high latitudes). However, a limited number of palaeoclimate studies for the mid Holocene have sought to corroborate field evidence with model outputs in New Zealand, one of few locations in the Southern Hemisphere with abundant terrestrial proxy data (McGlone et al., 1993). In addition, current hypotheses seeking to link insolation controls and regional climate variability across Milankovitch timescales for New Zealand (Vandergoes et al., 2005) require further testing. Therefore scrutiny of critical late-Quaternary periods for proxy/model comparisons in New Zealand is warranted.

The mid Holocene also provides a useful study period for testing the capability of General Circulation Models (GCMs) to represent the effects of perturbing the seasonal insolation characteristics on New Zealand climate. This time slice is recent enough that global sea level and continental geometry can be

assumed to be akin to the present, and there are significant proxy data available locally for making comparisons with palaeoclimate outputs (Li et al., 2008; Lorrey et al., 2010; McGlone et al., 1993). However, while GCMs provide useful information on large-scale circulation pattern changes, their spatial resolution is too coarse to adequately resolve the complex topographical features of New Zealand. This can be seen by comparing Figures 1(a) and (b). As New Zealand is located within the main Southern Hemisphere mid-latitude westerly wind belt, the surface topography has a strong influence on local-scale climate. For example, there are strong east–west temperature and precipitation gradients across the mountainous South Island,

<sup>1</sup>National Institute of Water and Atmospheric Research (NIWA), Wellington, New Zealand

<sup>2</sup>National Institute of Water and Atmospheric Research (NIWA), Auckland, New Zealand

<sup>3</sup>Victoria University of Wellington, New Zealand

<sup>4</sup>Climate Change Research Centre, University of New South Wales, Australia

<sup>5</sup>ARC Centre of Excellence for Climate System Science, University of New South Wales, Australia

<sup>6</sup>Helmholtz-Zentrum Geesthacht, Centre for Materials and Coastal Research, Institute for Coastal Research, Germany

<sup>7</sup>School of Environment, The University of Auckland, New Zealand

<sup>8</sup>Monash Weather and Climate, Monash University, Australia

## Corresponding author:

Duncan Ackerley, Monash Weather and Climate, Monash University, Clayton, Victoria 3800, Australia.

Email: duncan.ackerley@monash.edu

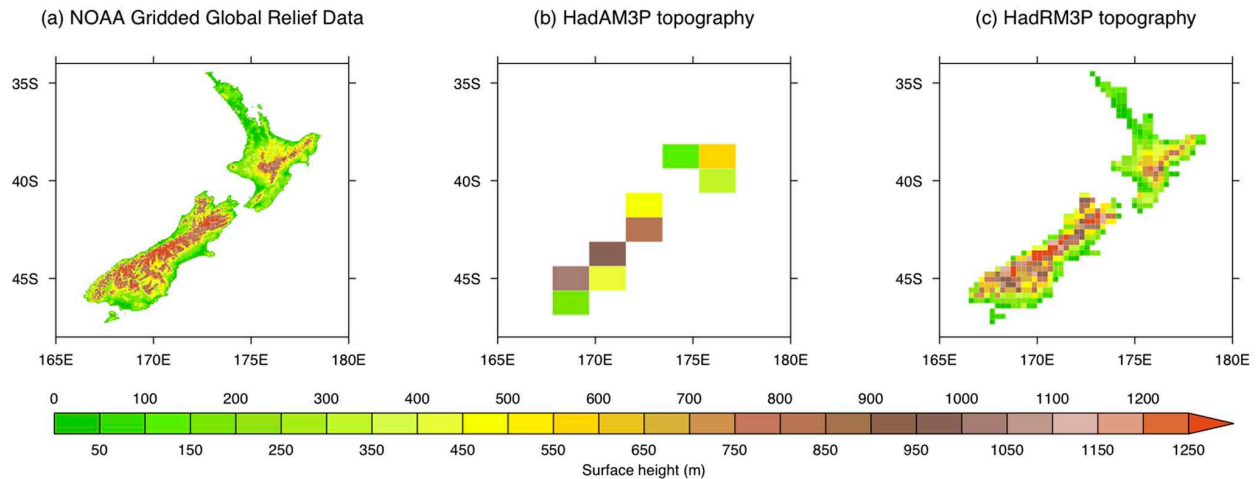


**Figure 1.** Land surface height above mean sea level (m) taken from (a) ETOPO2v2 Global Gridded 2-minute Database, National Geophysical Data Center, National Oceanic and Atmospheric Administration, US Department of Commerce, <http://www.ngdc.noaa.gov/mgg/global/etopo2.html>, (b) the GCM and (c) the RCM used in this study.

which acts as a barrier to the westerly flow (see Salinger, 1980a, 1980b; Salinger and Mullan, 1999). Therefore, a higher-resolution model capable of representing the complex surface topography of New Zealand may capture some of the local-scale diversity in climate.

In order to represent the local-scale diversity in climate, regional climate models (RCMs) have been used and evaluated to give high-resolution output for past, present and future climate for different parts of the world (Ackerley et al., 2011b; Christensen et al., 2010; Drost et al., 2007; Gómez-Navarro et al., 2011; Rummukainen, 2010; Strandberg et al., 2011). The use of RCM simulations for New Zealand has been undertaken previously in Ackerley et al. (2012) who demonstrated that the spatial correlations between the time-averaged (annual and seasonal) climate components agree very well with the contemporary observational record. For example the RCM is able to capture the strong west to east precipitation gradient across the mountainous South Island, and also represents the colder surface air temperatures that are prevalent in alpine reaches of both the North and South Islands. This is primarily due to the land surface height used by the RCM, which displays more of the topographical diversity apparent over the New Zealand land-mass than in a GCM (compare Figures 1a and 1c). Therefore, the use of a high-resolution RCM, forced by boundary conditions from a free running and/or externally forced atmosphere–ocean GCM, can be employed to undertake dynamical downscaling of the large-scale atmospheric flow to better represent New Zealand climate.

While a high-resolution RCM is capable of resolving the local-scale features of New Zealand climate, there are systematic biases that are idiosyncratic to any model (see Ackerley et al., 2012). Therefore an ensemble of simulations using a variety of perturbations to the boundary conditions and model physics enables the possibility of differentiating between real and model-specific climate anomalies (Ackerley et al., 2011a; Braconnot et al., 2007a, 2007b; Rojas and Moreno, 2010). The aim of this study is to identify robust differences between the mid Holocene (c. 6000 yr BP) and pre-industrial (c. AD 1750) climates of New Zealand using an ensemble of GCM and RCM simulations forced by different boundary conditions. All reference to the seasons will be December–February (DJF), March–May (MAM), June–August (JJA)

and September–November (SON) for austral summer, autumn, winter and spring, respectively.

## Model setup and experiments

To obtain high-resolution surface air temperature and precipitation data, this study makes use of the Hadley Centre Regional Model (HadRM3P, Jones et al., 2004) nested inside the Hadley Centre Atmospheric Model version 3 (HadAM3P, Pope et al., 2000). The horizontal resolution of HadRM3P is  $0.27^\circ$  latitude and longitude (approximately 30 km) whereas the horizontal resolution of HadAM3P is  $1.25^\circ$  latitude by  $1.875^\circ$  longitude (more than 100 km grid spacing). The higher resolution of HadRM3P allows the interaction between the atmospheric circulation and New Zealand's complex topography to be represented more accurately than in the lower resolution HadAM3P. Details and references pertinent to HadRM3P's performance in comparison with data from the Virtual Climate Station Network (VCSN, see Tait, 2008; Tait et al., 2006) and the parameterized processes can be found in Ackerley et al. (2012).

To undertake these experiments, HadAM3P and HadRM3P need to be run with insolation, greenhouse gas concentrations and sea surface temperatures (SSTs) that are representative of the pre-industrial period and 6000 yr BP. The insolation specifications follow those of the Paleoclimate Modelling Intercomparison Project 2 (PMIP2) as given in Braconnot et al. (2007a). The anomaly in insolation for the Southern Hemisphere (SH) for the 6000 yr BP simulations compared with the pre-industrial control simulations can be seen in Figure 2. Most of the SH receives less insolation from December through to June with more insolation from July to November, indicating weaker seasonality at 6000 yr BP.

The specifications for greenhouse gas concentrations also follow the PMIP2 setup (Braconnot et al., 2007a) with the pre-industrial carbon dioxide ( $\text{CO}_2$ ), methane ( $\text{CH}_4$ ) and nitrous oxide ( $\text{N}_2\text{O}$ ) concentrations set to 280 ppmv, 760 ppbv and 270 ppbv, respectively. The levels of  $\text{CO}_2$  and  $\text{N}_2\text{O}$  remain unchanged in the PMIP2 6000 yr BP simulations, however the levels of  $\text{CH}_4$  are reduced to 650 ppbv. These greenhouse gas concentrations are used for the pre-industrial and 6000 yr BP simulations below.

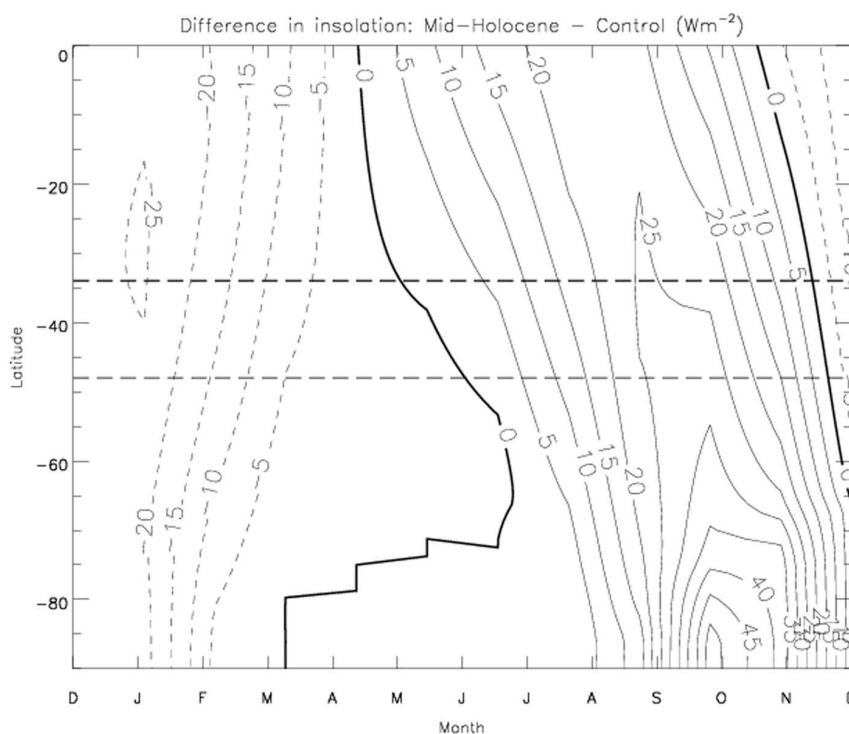


**Figure 2.** The difference in incoming solar radiation (insolation) at the top-of-the-atmosphere for the mid-Holocene simulations relative to the pre-industrial simulations ( $\text{W/m}^2$ ). The long-dashed, horizontal lines indicate the northern and southern extents of the New Zealand land mass.

HadAM3P does not include a fully dynamical ocean and uses only prescribed SSTs and sea-ice concentrations. The SSTs, therefore, are specified from simulations where an oceanic response has been generated from the different radiative fluxes, forced by the insolation and greenhouse gas concentrations specified above. The SST values are derived from the pre-industrial and 6000 yr BP simulations of the models used in Ackerley et al. (2011a). The models used to derive the SST originally are CSIRO Mk3L (Phipps et al., 2011, 2012), ECHO-G (Legutke and Voss, 1999; Wagner et al., 2007), HadCM3\_UB (Gordon et al., 2000; Singarayer and Valdes, 2010) and MIROC (K-1 Model Developers, 2004; Ohgaito and Abe-Ouchi, 2007). Each of these model simulations employs a fully dynamical ocean coupled to the atmosphere, which responds to the insolation and greenhouse gas forcings of the pre-industrial and 6000 yr BP boundary conditions. The absolute SSTs were taken from the pre-industrial and 6000 yr BP simulations of CSIRO MK3L, ECHO-G, HadCM3\_UB and MIROC, and averaged for each month of available data (100 years in all cases except ECHO-G which had 50 years of data) to give eight different monthly-mean, climatological SST fields (two from each model). These climatological SST fields are then bi-linearly interpolated to match the model grid resolution of HadAM3P. Eight simulations of HadAM3P are run using those prescribed climatological SSTs as the lower boundary conditions with the SST repeated cyclically every 12 months. Each simulation is run for 31 years, with the first year regarded as the spin up and subsequently removed from the analysis. While this method will remove any modes of interannual and decadal variability, any differences in the mean state of the SST fields will be represented at the models' lower boundary and subsequently influence the simulated mean climate state. The differences in seasonal mean SST for each of the 6000 yr BP simulations relative to the pre-industrial can be seen in Figure 3. There are obvious differences in each of the SST fields used for each pair of simulations; however, there are some important similarities.

The SST anomalies are at their largest negative values in MAM and JJA, which follow the largest negative anomalies in the 6000 yr BP insolation (relative to the pre-industrial) shown in Figure 2. This time lag between the largest negative insolation and the SST anomalies is likely to be due to the thermal inertia of the oceans in the original GCM simulations (which used fully dynamical oceans). Similarly, the largest positive SST differences occur in SON (and to a lesser extent DJF) as a lagged response of the ocean to the higher insolation (Figure 2). A similar effect of a delayed oceanic response to changes in orbital forcing during the mid Holocene has also been reported for the high-latitude Northern Hemisphere, which is caused by a lagged sea-ice response (see Renssen et al., 2005).

The same method described above is applied to produce the HadRM3P SST fields with the global SSTs (from the original coupled ocean–atmosphere GCM simulations) both extrapolated over the land–sea mask and then interpolated to the resolution of HadRM3P. The SSTs used in the HadRM3P domain are then separated from the global field and the HadRM3P land surface (see Figure 1c) is masked over the SSTs. This is repeated for all eight of the SST fields described above. While this method gives a highly smoothed representation of the SST in the New Zealand region, any differences in SST within the local vicinity of New Zealand would be included and may influence the local climate. This implementation is common in RCM studies because most RCMs do not consist of a dynamical oceanic component and therefore the lower boundary forcing is taken from a driving GCM.

## Results

### Surface air temperature at 1.5 m

The ensemble-mean difference in surface air temperature ( $T_{\text{as}}$ ) can be seen in Figure 4 for each season and the overall 'annual' mean along with the corresponding grid-point standard deviations

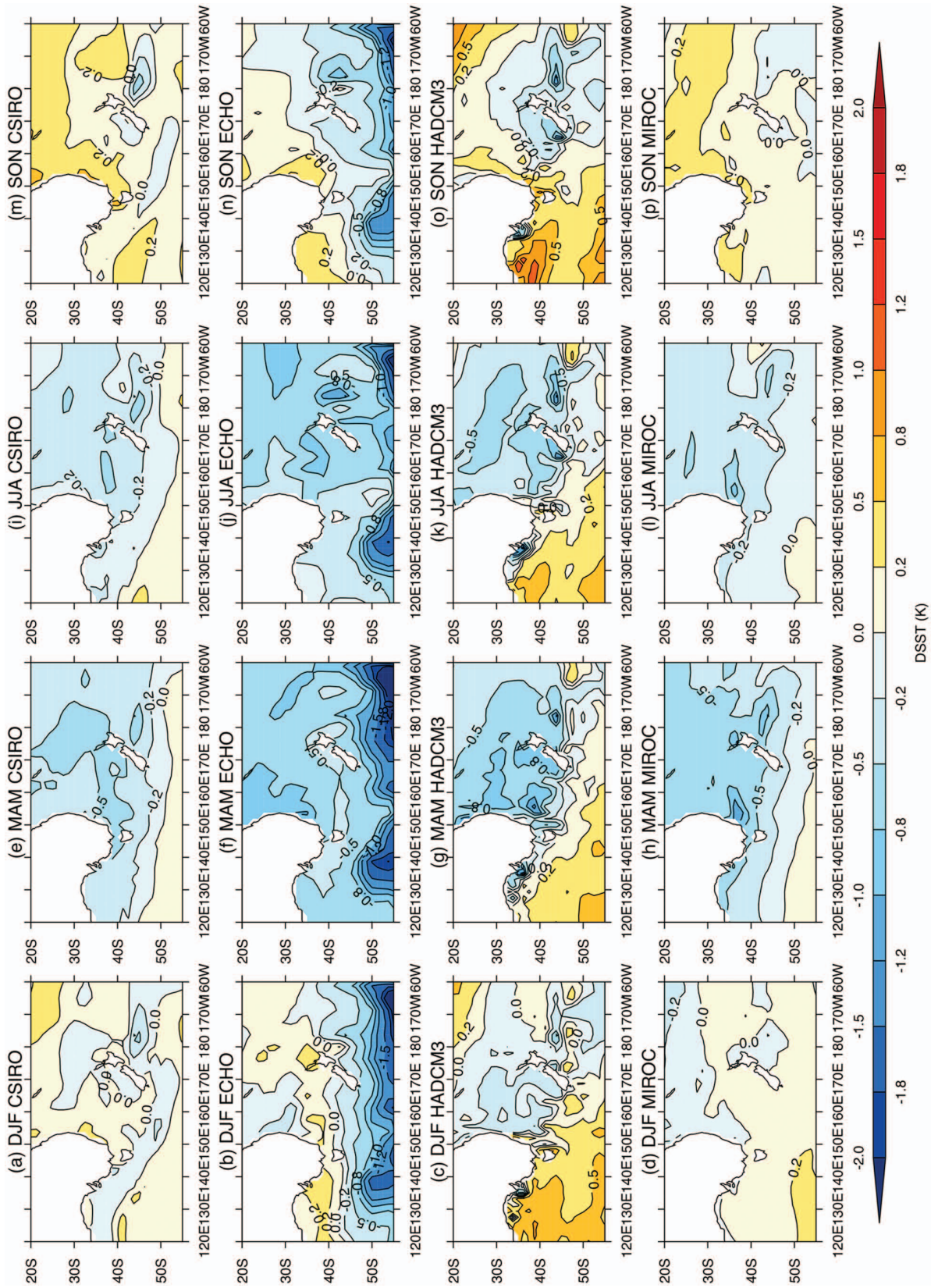


**Figure 3.** The seasonal mean difference in SST for the 6000 yr BP simulations relative to the pre-industrial simulations ( $^{\circ}\text{C}$ ) for (a)–(d) DJF, (e)–(h) MAM, (i)–(l) JJA and (m)–(p) SON. The original GCM from which the SST were provided are also labelled as CSIRO (CSIRO Mk3L), ECHO (ECHO-G), HADCM3 (HadCM3\_UB) and MIROC (MIROC).

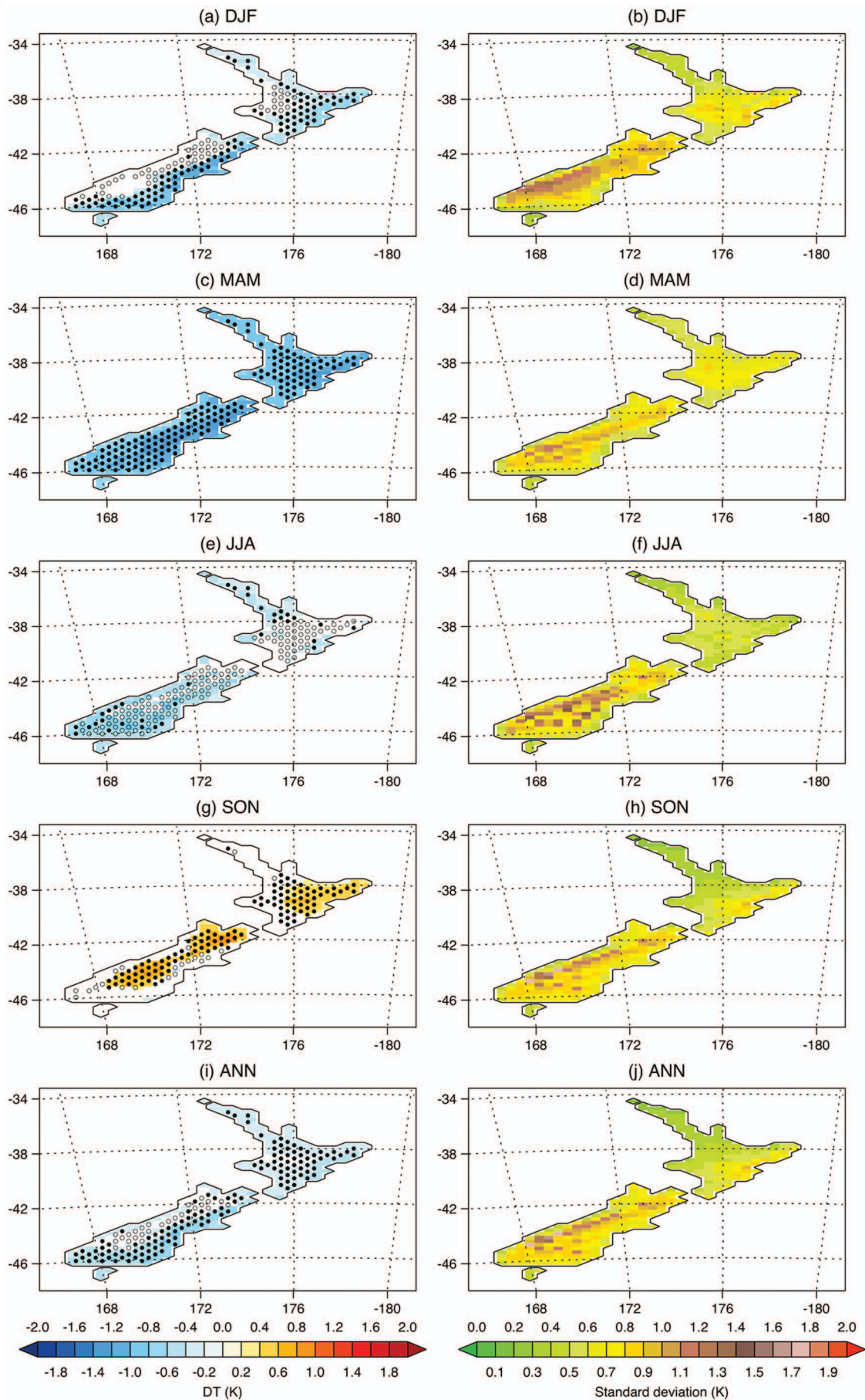


**Figure 4.** The difference in surface air temperature at 1.5 m ( $T_{as}$ ) for the mid-Holocene RCM simulations relative to the pre-industrial simulations (K) averaged over all four pairs of model simulations (left column) and the standard deviation in the seasonal mean temperature differences across all four models (K, right column) for (a–b) DJF, (c–d) MAM, (e–f) JJA, (g–h) SON and (i–j) the annual (ANN) mean change. Only statistically significant changes ( $p \leq 0.05$ ), using a two-sample  $t$ -test for equal means, are shaded for the ensemble mean differences. Stippling indicates where three (open circles) or four (solid circles) of the simulations agree on the sign of the simulated change.

of those changes taken across all four simulations. Also plotted in Figure 4 are the locations of grid points where either three or four of the simulations agree on the sign of the mean  $T_{as}$  differences.

DJF, MAM and JJA are generally colder at 6000 yr BP than the pre-industrial and in many areas at least three of the four simulations agree on the sign of the difference in temperature (Figure 4a, c and e). The corresponding standard deviations (Figure 4b, d and f) are also smaller in magnitude than the mean difference in the ensemble mean temperature except in the western South Island in DJF, where the temperature differences are not statistically significant and model agreement is poor. The SST differences (for 6000 yr BP relative to pre-industrial) in each of the simulations differ in sign along the west coast of the South Island (and more widely into the Tasman Sea to the east, Figure 3a–d), which is likely to be responsible for some of the disagreement in DJF. In MAM and JJA the SST are colder in the 6000 yr BP simulations in most of the ocean surrounding New Zealand. In combination with the reduced insolation, this may cause the more uniform lower temperatures across the modeled land surface.

The strongest differences in  $T_{as}$  occur in MAM (Figure 4c) where there is also very strong model agreement. Also, the grid-point values of the standard deviations across the models are small (Figure 4d) relative to the ensemble mean, which further indicates strong agreement on the MAM cooling in all four models. This coincides with the largest negative SST differences for 6000 yr BP relative to the pre-industrial (Figure 3).

Unlike December to August, warmer conditions are simulated to have prevailed across some regions in New Zealand during SON (Figure 4g) but the high standard deviations across the ensemble (Figure 4h) relative to the ensemble mean change, reduce the confidence in the result. Again, the uncertainty in coastal areas is likely to be the result of the differences in SST between the 6000 yr BP and pre-industrial simulations, which have opposing signs close to New Zealand (see Figure 3m–p). However, SON is distinctly different from the other seasons presented in Figure 4 and suggests that, despite some disagreement between the models, temperatures were unlikely to have been cooler at 6000 yr BP than for the pre-industrial in this season. Neither were they necessarily much warmer, despite the stronger insolation (see Figure 2). The regions with the largest differences in  $T_{as}$  also have strong model agreement (Figure 4g), which suggests that the mechanisms causing SON climate to be relatively warmer than in the other seasons are represented in each simulation.

While the results in Figure 4 highlight where the largest ensemble mean differences in temperature occur and whether those changes are large or small relative to the spread across the simulations, they do not indicate how well the spatial pattern of these differences compare between individual simulations. In order to address this, the pattern correlations of temperature across the modelled New Zealand land mass are given for each season and annually in Table 1. High correlations occur between each of the models in DJF, which indicates the models are in strong agreement on the spatial distribution of the temperature changes in Figure 4a. Despite the strong model agreement on general cooling across New Zealand in MAM, the pattern correlations are weaker than those of DJF, which indicates that the pattern of cooling across the land mass differs somewhat between the models. JJA has the weakest spatial correlations, which agrees with the weaker model agreement in Figure 4e and there are very few grid points where all four models agree on the sign of the

temperature differences. In SON however, the spatial correlations are much higher despite smaller areas of model agreement compared with DJF or MAM (compare Figure 4a, c and g). The strong SON correlations indicate that while much of the land surface temperature may not have changed significantly, the simulations agree well on those areas that have higher temperatures and those with little change. Finally, the annual mean pattern correlations are also very high, which indicates that the models agree well on the spatial differences in temperature for 6000 yr BP relative to the pre-industrial.

Overall, as the majority of the seasons were simulated as being cooler for 6000 yr BP relative to the pre-industrial simulations, the annual mean change also suggests cooler temperatures dominated throughout much of New Zealand (Figure 4i) with strong statistical significance in many areas ( $p < 0.05$ ) and strong model agreement in most areas. The small values of the across-model standard deviations (Figure 4j) further suggest that there is good agreement across the models for cooler conditions at 6000 yr BP relative to the pre-industrial and the high pattern correlations for the annual mean (Table 1) indicate good spatial agreement.

### Precipitation

The seasonal and annual mean change in precipitation for the ensemble mean and the standard deviations in the across-ensemble mean change in precipitation (relative to the pre-industrial simulations) can be seen in Figure 5. The statistically significant changes in precipitation are similar in DJF and MAM (Figure 5a and c), with less precipitation in the western South Island and more in eastern areas of both islands and strong model agreement in both of these areas at 6000 yr BP. However, the grid-point standard deviations of these changes, particularly in the North Island, are large relative to the mean change and indicate a large spread in the simulated rainfall in both seasons (Figure 5b and d). The higher variability in precipitation relates to the processes involved in the generation of precipitation and the specific atmospheric flow conditions in the driving GCM. For instance, comparatively small changes in the driving GCM can have pronounced influence on the resulting precipitation pattern, especially in the vicinity of mountain ranges (for example see Pfeiffer and Zängl, 2011, for the European Alps).

In JJA (Figure 5e), the majority of the North Island is wetter (statistically significant) in the ensemble mean with very little change in South Island precipitation, with a North Island/South Island split on good versus weak model agreement. Also, while the across-model standard deviations are generally at their smallest of all seasons in JJA (Figure 5f), they are still equal-to or larger-than the ensemble mean changes indicating some uncertainty.

The SON changes in precipitation (Figure 5g) are negative throughout much of the central and northern South Island and the northeastern North Island with more precipitation in the southeastern South Island. At least three of the four models agree on the lower (higher) precipitation in the North Island and central South Island (southeastern South Island). Again, the across-model standard deviation is larger-than or equal-to the ensemble mean changes (Figure 5h), reducing the confidence in the ensemble mean change.

The annual mean changes (Figure 5i) suggest that drier conditions prevailed in parts of the western South Island with wetter conditions to the east of both islands (similar to DJF and MAM).

**Table 1.** Spatial correlations for the 6000 yr BP minus pre-industrial simulations for surface air temperature and precipitation (*italics*) for each simulation relative to another. Statistically significant ( $p \leq 0.05$ ), positive correlations are in bold type.

Season	Model	CSIRO Mk3L	ECHO-G	HadCM3_UB	MIROC
DJF	CSIRO Mk3L	<b>X</b>	<b>0.91</b>	<b>0.84</b>	<b>0.24</b>
DJF	ECHO-G	<b>0.89</b>	<b>X</b>	<b>0.89</b>	<b>0.36</b>
DJF	HadCM3_UB	<b>0.77</b>	<b>0.61</b>	<b>X</b>	<b>0.45</b>
DJF	MIROC	<b>0.87</b>	<b>0.84</b>	<b>0.51</b>	<b>X</b>
MAM	CSIRO Mk3L	<b>X</b>	<b>0.47</b>	<b>0.89</b>	-0.37
MAM	ECHO-G	<b>0.59</b>	<b>X</b>	<b>0.46</b>	0.07
MAM	HadCM3_UB	<b>0.73</b>	<b>0.17</b>	<b>X</b>	<b>0.48</b>
MAM	MIROC	<b>0.42</b>	<b>0.56</b>	<b>0.23</b>	<b>X</b>
JJA	CSIRO Mk3L	<b>X</b>	<b>0.88</b>	-0.71	-0.38
JJA	ECHO-G	<b>0.15</b>	<b>X</b>	-0.75	-0.39
JJA	HadCM3_UB	-0.17	-0.09	X	<b>0.78</b>
JJA	MIROC	-0.43	<b>0.34</b>	<b>0.54</b>	<b>X</b>
SON	CSIRO Mk3L	X	<b>0.28</b>	-0.41	<b>0.48</b>
SON	ECHO-G	<b>0.88</b>	<b>X</b>	<b>0.22</b>	<b>0.57</b>
SON	HadCM3_UB	<b>0.75</b>	<b>0.68</b>	X	<b>0.30</b>
SON	MIROC	<b>0.81</b>	<b>0.89</b>	<b>0.44</b>	<b>X</b>
ANN	CSIRO Mk3L	<b>X</b>	<b>0.63</b>	<b>0.36</b>	<b>0.60</b>
ANN	ECHO-G	<b>0.87</b>	<b>X</b>	<b>0.17</b>	<b>0.57</b>
ANN	HadCM3_UB	<b>0.75</b>	<b>0.68</b>	<b>X</b>	<b>0.30</b>
ANN	MIROC	<b>0.81</b>	<b>0.89</b>	<b>0.44</b>	<b>X</b>

The model agreement on the annual mean changes in precipitation is weaker than for  $T_{as}$ ; however, at least three of the simulations agree on the sign of the grid point precipitation change where they are statistically significant. The across-model standard deviations are also smaller than or comparable with the ensemble mean changes (Figure 5j), which indicate a higher degree of model agreement for the annual mean changes than for any individual season. Therefore, western (eastern) areas may have been drier (wetter) at 6000 yr BP relative to the pre-industrial with the strongest seasonal changes occurring in DJF and MAM (which influence the annual mean).

As with  $T_{as}$ , the spatial correlations of the differences in precipitation between each of the models can be seen in Table 1 (*italics*). The strongest spatial agreement occurs in DJF, which indicates that the dry southwest/wet east and north pattern in Figure 5a is common to all of the models; however, the correlation is weaker for the MIROC SST simulation and is an outlier relative to the other models. The spatial correlations are also high for the MAM differences (albeit weaker than for DJF), with the exception of the MIROC SST simulation. The cause of the weaker correlations is associated with a general increase in precipitation throughout New Zealand in the MIROC SST simulation whereas the other three simulations have the dry west/wet north and east pattern (not shown), which can be seen in the ensemble mean (Figure 5c). The weakest correlations (and strongest anti-correlations) occur during JJA, which has the weakest model agreement on the sign of the precipitation differences over much of New Zealand (Figure 5e). The individual simulations agree on the higher North Island precipitation but there is large disagreement on the South Island precipitation (not shown) and it is therefore difficult to have any confidence in the simulated differences in precipitation during JJA. In SON the pattern correlations (as with  $T_{as}$ ) are much stronger, which suggests that the pattern of lower (higher) precipitation in the central South Island (southeast South Island) in Figure 5g is common across each of the simulations (with the exception of HadCM3\_UB). Finally, the annual mean correlations are high between each of the simulations. This suggests that

the simulated differences in annual mean rainfall for 6000 yr BP relative to the pre-industrial share common spatial characteristics. However despite some of the commonality, the seasonal changes in precipitation are still highly variable between the simulations and therefore highly uncertain. This in turn suggests a strong dependency of the regional climate model on the driving lower boundary conditions and respective atmospheric circulation. Therefore changes in atmospheric circulation might have a more profound influence on precipitation than on surface air temperatures, because the processes controlling precipitation variability can act on temporally and spatially different scales.

### Circulation

The circulation patterns modelled for NZ (see Figure 6) suggest anomalous easterly and southeasterly quadrant flow during DJF and MAM, with lower pressure north of the country and a shallower circumpolar trough (6000 yr BP relative to the pre-industrial). This pattern also implies weaker westerly flow in general at 6000 yr BP. In addition, intensification of 'high' pressure over and to the east of NZ during JJA and SON, respectively, suggests more settled conditions occurred during those two seasons at 6000 yr BP. During SON in particular, weaker westerlies (evidenced by a shallower circumpolar trough and weaker subtropical high pressure) and increased anticyclonic conditions are implicated by the surface pressure patterns, which are reminiscent of the negative polarity of the Southern Annular Mode (SAM, Thompson and Wallace, 2000). The anomalous easterly/southeasterly flow agrees with the precipitation responses for the annual mean given in Figure 5.

## Discussion

### Why was New Zealand generally colder in the mid Holocene?

Modern climatological studies suggest the combination of insolation forcing, seasonally varying SST characteristics surrounding

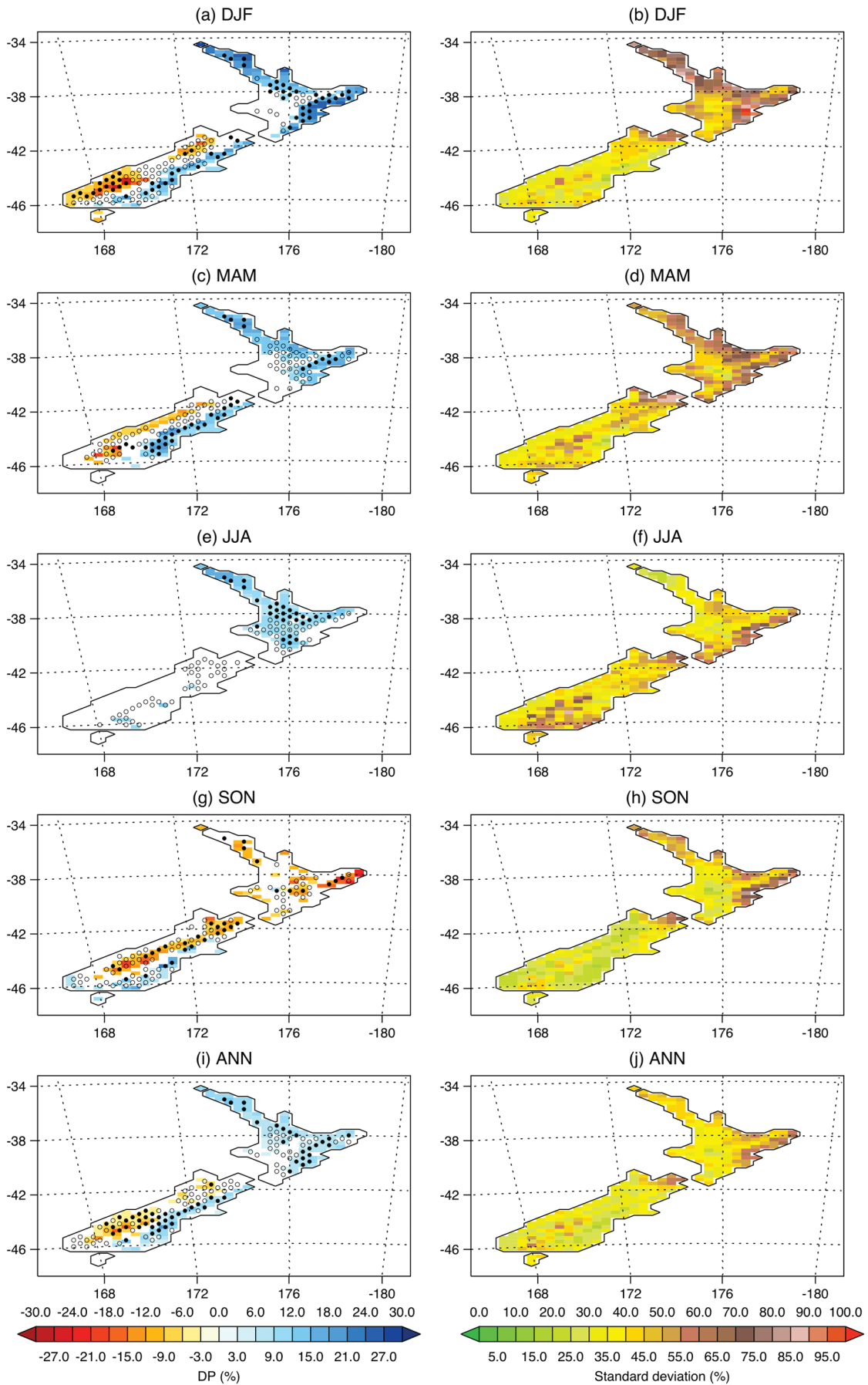


**Figure 5.** The difference in precipitation for the mid-Holocene RCM simulations relative to the pre-industrial simulations (%) averaged over all four pairs of model simulations (left column) and the standard deviation in the seasonal mean precipitation differences relative to the pre-industrial control simulations across all four models (%), using a two-sample *t*-test for equal means, are shaded for the ensemble mean differences. Stippling indicates where three (open circles) or four (solid circles) of the simulations agree on the sign of the simulated mean differences.

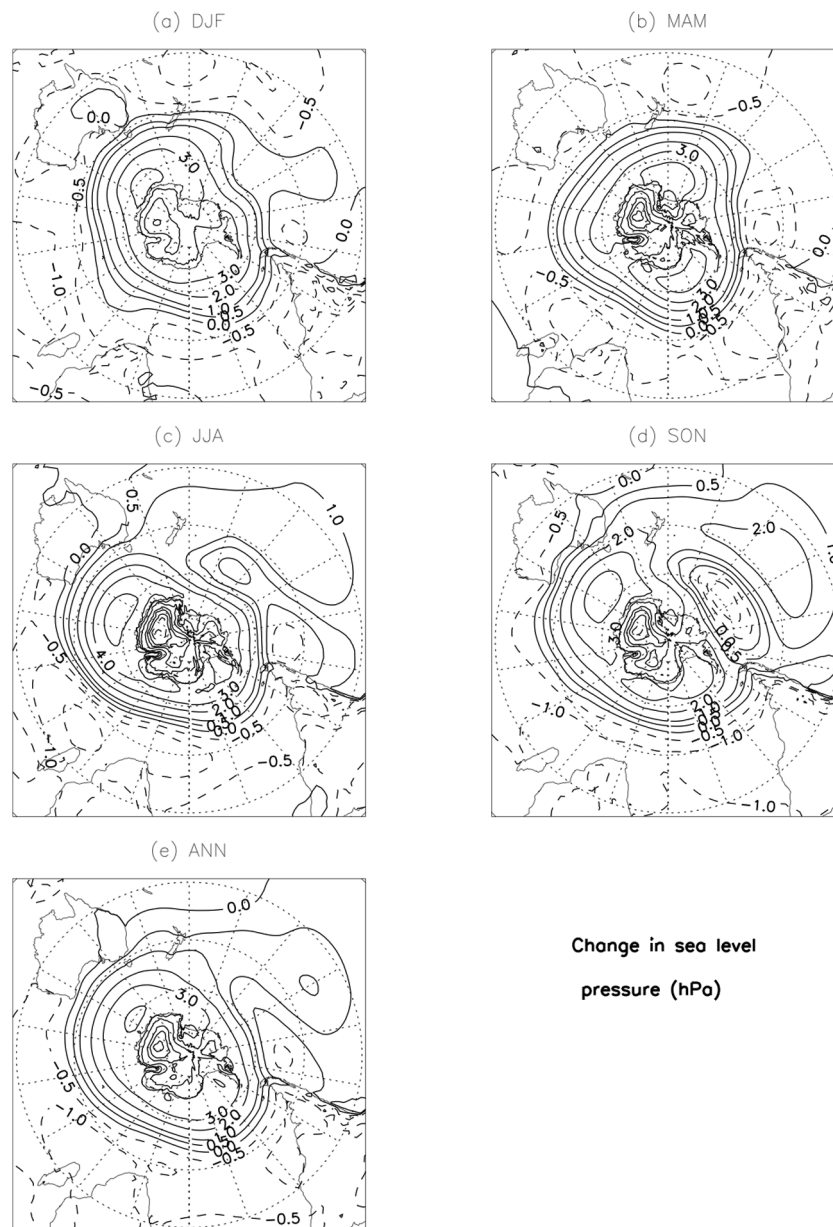


**Figure 6.** The difference in sea level pressure (SLP) for the mid-Holocene GCM simulations relative to the pre-industrial simulations (hPa) averaged over all four pairs of model simulations for (a) DJF, (b) MAM, (c) JJA, (d) SON and (e) the overall annual mean change.

New Zealand, and the direction of incident wind flow across the country are all important contributors that dictate terrestrial temperature characteristics (see Kidson, 2000; Kidston et al., 2009; Mullan, 1998; Renwick, 2011; Salinger and Mullan, 1999). In the case of the 6000 yr BP simulations we might simply expect the New Zealand values of  $T_{as}$  to be cooler in DJF and MAM, and warmer in JJA and SON from the insolation changes in Figure 2. However, the analysis in Section ‘Surface air temperature at 1.5 m’ suggests that insolation differences are not the only explanation for the changes, with reduced values of  $T_{as}$  in DJF, MAM and JJA and warmer temperatures in SON. Therefore it appears that other influences on  $T_{as}$  may be the result of both some lag in the climate system (for example the seasonal changes in SST lag the seasonal changes in insolation because of the ocean’s thermal inertia) and local-scale, topographical interactions with atmospheric circulation anomalies.

During SON, the stronger insolation is likely to be the main driver behind the higher values of  $T_{as}$  in the model simulations.

Also, despite a mixture of cooler and warmer SSTs surrounding New Zealand in the 6000 yr BP model simulations (Figure 3m–p), the SSTs in the southwest Pacific are at their most similar to the pre-industrial simulation with the weakest negative differences. However, the presence of much cooler SSTs surrounding New Zealand in two simulations and the prevalence of anomalous southerly and southeasterly flow (see Figure 6d) may account for the weaker changes in temperature in parts of the South Island. There is also evidence for an increase in cloud cover in the eastern South Island (not shown), which corresponds with the anomalous southerly/southeasterly flow and may contribute to the weaker temperature differences there.

For DJF, the strongest reductions in insolation at 6000 yr BP occur during January and February (Figure 2), which is likely to have a significant cooling influence on the land temperatures. However, the simulated pattern is not uniform across the land surface, which indicates that other factors are influencing  $T_{as}$ . While the negative SST differences are stronger in DJF than SON, there are

still areas with slightly warmer SSTs within close proximity to New Zealand (Figure 3a–d). These warmer SSTs prevail from SON, despite the relatively lower insolation during DJF at 6000 yr BP. Again, this is associated with the thermal inertia of the ocean, which causes the differences in SST to lag the insolation differences.

Overall, colder New Zealand DJF temperatures in northern and eastern regions and near normal temperatures in western areas for 6000 yr BP (Figure 4a) can be explained by a combination of differences in cloud cover (cloud cover increases slightly, not shown) and surface moisture availability from higher precipitation (Figure 5a), which result from the anomalous easterly flow. Also, the presence of slightly cooler SSTs offshore of the South Island in all simulations will contribute to cooling in the eastern South Island. The suggestion of easterly anomalies in this circumstance is also supported by the model-based precipitation results (Figure 5a) indicative of a strong east–west precipitation gradient spanning the long axis of the Southern Alps. Near normal temperatures in the western South Island during this particular season are different from the rest of New Zealand, and reflect a balance between the differences in the SST fields, the effects of lowered insolation and the Foehn warming that can occur under enhanced easterly flow.

The largest reduction in  $T_{as}$  is observed in MAM (New Zealand mean change  $-0.96^{\circ}\text{C}$ ; Figure 4b) and corresponds with the largest negative differences in the SSTs (Figure 3e–h). This occurs during a period where the insolation is still lower in the 6000 yr BP simulations than the pre-industrial simulations but follows directly after the strongest reduction in SH insolation (February, see Figure 2). However, as the MAM reduction in  $T_{as}$  also does not correspond with the period when the largest reductions in insolation occur in the New Zealand sector (January–February, see Figure 2), this reinforces the suggestion that a lagged response between insolation and New Zealand  $T_{as}$  also exists, and there is a link between land and SST anomalies. Despite some similarity between the MAM and DJF circulation patterns, the MAM flow was anomalously southeasterly (Figure 6b), and in combination with some of the coldest SST anomalies offshore of both the North and South Islands (Figure 3e–h), this helps to explain the overall coldest terrestrial temperature anomalies during MAM in the 6000 yr BP simulations.

During JJA the insolation is slightly higher, but the  $T_{as}$  values are lower in the 6000 yr BP simulation than the pre-industrial control simulation. Similarly, even though there is slightly more insolation during JJA in the 6000 yr BP simulation (compared with the pre-industrial) the SSTs are generally cooler in all of the 6000 yr BP simulations (Figure 3i–l), which are likely to be an important influence on the lower values of  $T_{as}$  seen in Figure 4b.

Overall, the relative trend in insolation (a continued increase from February through to November) indicates that the timing of the SST changes consistently lag behind insolation shifts. This suggests an orbitally driven solar forcing mechanism that influences the development of SST anomalies that in turn reinforce circulation patterns that elicit land-based climate anomalies. The long fetch over the open ocean surrounding New Zealand means regional SST characteristics would have been capable of imparting distinct traits onto incident air masses that contributed to the temperature anomalies over New Zealand at 6000 yr BP. These characteristics are further enhanced or reduced by the changes in insolation itself and locally induced circulation effects (such as cloud cover and the Foehn effect).

### Why does the precipitation change?

Distinct regional changes in precipitation for the 6000 yr BP simulations relative to the pre-industrial control are likely to be caused by atmospheric circulation anomalies across New Zealand (see Kidson, 2000; Kidston et al., 2009; Mullan, 1998; Renwick, 2011; Salinger and Mullan, 1999; for further details). The incident atmospheric flow, intersecting the long axial ranges that trend northeast–southwest, induces strong orographic rainfall effects, which cause the spatial differences seen in the model simulations.

In DJF and MAM there is relatively lower mean sea level pressure (SLP) to the north of New Zealand and higher SLP to the south, which suggests weakened westerlies (easterly anomalies) are related to the precipitation changes seen in Figure 5a and b, with wetter eastern and northern areas and drier in the western South Island. In JJA the difference in SLP is quite uniform across the country with an increase of approximately 1–1.5 hPa (Figure 6c). This is also reflected in the precipitation changes with little change except over the North Island where there are some small increases (Figure 5c). The differences in SLP in SON are very similar to those of JJA, except that the high anomaly to the southwest is centred more to the east in SON. This pattern results in a more southeasterly flow, with higher precipitation in southern and eastern parts of the South Island and drying across much of the rest of New Zealand. For the overall mean however, there is higher SLP encircling Antarctica, which leads to weaker westerly flow, indicative of the negative polarity of the SAM. The anomalous easterly flow leads to the eastern and northern areas of both islands being wetter, with drying in the western South Island (rain shadow in the lee of the Southern Alps).

### How do the RCM simulations compare with other modelling work?

Previous work by Ackerley et al. (2011a) used synoptic type classification to infer past climate regimes from GCM data. As the resolution of those models was too low to adequately resolve New Zealand's diverse topography, the differences in temperature and precipitation were inferred from SLP data that were classified into specific regime types (as done by Kidson, 2000). The suggestion was that, from December to May New Zealand would have been wetter (more trough-like), with drier conditions from June to November at 6000 yr BP, and little change in overall mean annual precipitation. The results of the Ackerley et al. (2011a) analysis also suggested that the North Island would have been warmer (cooler) and the South Island cooler (warmer) in MAM (SON), but that there would be little change in the overall mean temperature for 6000 yr BP relative to the pre-industrial. However, the temperature estimates in that study did not account for insolation or SST changes, and only took into account the changes in temperature that arose from differences in circulation modes (types). The use of the RCM here means that high-resolution model output can be used to estimate the changes in precipitation and temperature that result from the differences in insolation and SST, and the consequent differences in circulation that occurred in the 6000 yr BP simulations.

While higher precipitation was observed in DJF and MAM for the 6000 yr BP simulations, this occurred in eastern and northern areas of both the North and South Islands with lower or unchanged precipitation in the west of both islands. This is unlike the results

shown in Ackerley et al. (2011a), which suggested there was generally more precipitation throughout New Zealand during DJF and MAM. In SON, Ackerley et al. (2011a) suggested that New Zealand would be drier at 6000 yr BP, which agrees with the RCM output. However, Ackerley et al. (2011a) also suggested that JJA would be drier, which is not the case according to Figure 5c although there is disagreement across the simulations. The overall (annual mean) change in the RCM precipitation resembles the changes in DJF and MAM whereas Ackerley et al. (2011a) found there to be very little change in the annual mean precipitation. While there are some obvious differences between the estimations of Ackerley et al. (2011a) and the RCM simulations in this study, there are some similarities between both studies with wetter conditions (New Zealand mean) in DJF and MAM and drier conditions in SON. Ackerley et al. (2011a) was based on a statistical downscaling of GCM output, while these results are based on dynamical downscaling of GCM output. Hence, the results presented here represent an integration of the direct and indirect effects of insolation forcing, SST differences and circulation changes upon New Zealand surface climate, while Ackerley et al. (2011a) was purely circulation-based. However, the simulations undertaken in this study use the mean SST field derived by the models given in the Section 'Model setup and experiments' to drive both the GCM (HadAM3P) and the RCM (HadRM3P). Therefore the models are missing some of the interannual variability that may be important in governing the overall response of the precipitation. Also, there are biases associated with the structure of the parameterization schemes used in HadAM3P (see Pope et al., 2000, for a review of the performance of the lower-resolution HadAM3 model from which HadAM3P is derived) that may influence the circulation in the New Zealand sector despite using different SST fields in each simulation. The only way to formally test these hypotheses would be to use lateral boundary condition data derived directly from the forcing models given in the Section 'Model setup and experiments', or to repeat the regional modelling experiments using one or more alternative RCMs. However, this is not currently feasible and remains an area of future work.

As for  $T_{as}$ , the RCM-derived values differ greatly from the ones derived in Ackerley et al. (2011a). While the RCM includes the direct and indirect effects of both insolation, SST differences and circulation changes, the Ackerley et al. (2011a) method only accounted for the effects of changing the circulation. The model results in this study suggest that colder conditions prevailed from December to August with warmer conditions in SON in agreement with the results of Rojas and Moreno (2010). The use of the RCM therefore has provided further, high-resolution information about the seasonal and annual temperature characteristics of the climate at 6000 yr BP and improves upon the estimates in Ackerley et al. (2011a). However, as stated above for precipitation, there may be circulation biases in HadAM3P that are contributing to the differences between this study and Ackerley et al. (2011a). Since the insolation is such a large driving factor behind the results presented here, and as the method used in Ackerley et al. (2011a) cannot account for the direct impacts of such changes, the results of the RCM simulations should provide a better estimate of the changes in temperature for 6000 yr BP relative to the pre-industrial. Southern Hemisphere PMIP2 simulation results presented by Rojas and Moreno (2010) indicate seasonal circulation patterns similar to those shown in this study, with weaker westerly winds (anomalous easterlies) and cooler overall temperatures at approximately 6000 yr BP across New Zealand. The basic

model similarities between this study and previous work by Rojas and Moreno (2010) with increased precipitation in DJF and MAM and reduced precipitation in JJA and SON combined with generally lower temperatures throughout the year except SON (in the New Zealand sector for 6000 yr BP relative to the pre-industrial) is very encouraging. This suggests that statistical downscaling approaches may be limited in their application to profoundly changed climatic states.

#### How do the results compare with proxy data?

As recently summarized in Ackerley et al. (2011a), and noted by previous researchers (Li et al., 2008; McGlone et al., 1993), a significant climate shift is postulated for New Zealand during the mid Holocene. Multiple environmental reconstructions have suggested that a New Zealand-wide circulation change altered regional temperature and precipitation characteristics at that time. Lorrey et al. (2010) recently examined the mid-Holocene palaeoprecipitation evidence for the country and, on the basis of many records, suggest that a change from more frequent blocking to more frequent zonal flow occurred close to 6000 yr BP. This conclusion, supporting the assertions of Li et al. (2008) and McGlone et al. (1993), was based largely on speleothem  $\delta^{13}C$  (palaeowater balance) signals (see Lorrey et al., 2008, 2011 and Williams et al., 2010 for explanation of speleothem stable isotope signals) and supporting archives that illustrated wet conditions for northern and eastern regions, and dry conditions for the western South Island.

Notable reductions in the abundance of the frost-tender species *Ascarina lucida* and changes in peat deposition at Sponge Swamp in the western South Island (Li et al., 2008) follow the assertions of McGlone et al. (1993), who suggested mid-Holocene climate in northern and western areas of New Zealand shifted from more mild conditions toward wetter winters, slightly cooler temperatures, and more frequent southerly fronts and frosts (see McGlone and Topping, 1977; Martin and Ogden, 2002, 2005; Newnham et al., 1989 for explanations of the climatic affinity of *Ascarina*). Prior to the mid-Holocene shift, *Ascarina* pollen was also present and/or elevated at northern North Island sites, which suggests that regionally warm conditions and low frost occurrence existed broadly across NZ prior to the shift.

McGlone and Bathgate (1983) also note a marked increase in woody debris during the mid Holocene at a site in the southern South Island, and they suggested increased disturbance progressively ensued from this time because of the onset of more frequent westerly wind storms. While palaeocirculation studies are not so numerous for the mid Holocene in New Zealand, there is some very good evidence from past glacier activity that can also be used to corroborate the circulation changes that are implied by woody debris evidence. Tasman and Mueller glacier moraines, dated by cosmogenic radionuclides, suggest ice advances culminated close to 6520±360 years ago (Schaefer et al., 2009). These deposits are interpreted as a result of a circulation change that favoured lower temperatures in the western South Island (WSI) regional climate district (weighted to DJF, following the conclusions of Anderson and Mackintosh, 2006) and possibly accompanied by higher precipitation there.

Significant commonalities and key differences exist between the model results and proxy evidence. The exact timing of a mid-Holocene change is still obscure (and possibly asynchronous between regions) as a result of differing chronologic controls and

sample resolution employed on the proxy data archives. However when viewed from a multicentennial to millennial resolution, the proxy evidence suggests a mid-Holocene change did occur, and palaeoprecipitation patterns suggest wetter northern and eastern regions and a dry WSI prior to the shift (Lorrey et al., 2010). This is similar to the New Zealand precipitation signature offered by the RCM ensemble in this study (Figure 5), and supports the view that the RCM has faithfully captured the relative precipitation anomaly impacts of more frequent easterly circulation patterns. However the depiction of lower temperatures in three of four seasons and the annual mean of the model simulations appear akin to the palaeoclimate reconstruction spatial pattern for the time slice *after* the mid-Holocene shift (colder in all climate districts). The palaeotemperature pattern derived from the proxies is interpreted as being caused by a more westerly and southerly circulation regime (associated with trough conditions with important zonal contributions, see Renwick, 2011). The proxy–model discrepancy can be explained by the fact that the model simulation is centered on 6000 yr BP, and thus it may be depicting ‘the midst of a climate transition’ in the New Zealand sector of the SW Pacific. The chronologies for multiple palaeoclimate lines of evidence could also be improved to help clarify this discrepancy with additional radiocarbon dates. However, the joint model–proxy results suggest regional SST anomalies were forced by insolation that subsequently dictated New Zealand terrestrial temperatures.

#### *Dynamical interpretation of the results*

The implications of the explanation offered here are consistent with the interpretations offered in previous sections, and with a new SH palaeoclimate summation provided recently by Fletcher and Moreno (2011). They remark that a ‘steepening of the trans-Pacific SST gradient toward 7–6 ka in the Equatorial Pacific’ occurred, which may have been associated with stronger mid-latitude westerlies and more cold-water transport along the Chilean coastline in the eastern Pacific. Fletcher and Moreno (2011) also indicate that the resultant steepening of the trans-Pacific SST gradient would have helped to set up an enhanced Walker Circulation, an increase in El-Niño-Southern Oscillation (ENSO) intensity (Moy et al., 2002) and perhaps more frequent ENSO events in the mid Holocene (following Koutavas et al., 2006; Shulmeister, 1999). Following this sequence of events, characteristic circulation conditions may have been set up over New Zealand because of teleconnections with ENSO (and related low-frequency climate drivers such as the Interdecadal Pacific Oscillation (IPO)). This effect has previously been remarked on as a cause of past regional climate changes (Lorrey et al., 2010; McGlone et al., 1993). The similar timing of changes seen in many proxies across the Pacific Basin during the mid-Holocene transition could also reflect the onset of a large-scale, hemispheric circulation change, which may have significant ENSO and Southern Annular Mode (SAM) linkages. Fletcher and Moreno (2011) hypothesized that circulation-driven climate variability (for example ENSO, IPO, and SAM) may have dominated over insolation-driven climatic change towards the late Holocene. This may also explain why late-Holocene climate regime reconstructions for New Zealand, which reflect the regional atmospheric pressure anomaly patterns, show an intimate covariation of terrestrial precipitation and temperature signatures (Lorrey et al., 2008, 2010).

The suggestions made in this model–proxy intercomparison have exposed new caveats for Regional Climate Regime Classification

(see Lorrey et al., 2007, 2008, 2011). We suggest past circulation patterns established with that technique may be a novel way to verify both GCM and RCM model results for precipitation, but occasionally difficult to reconcile with terrestrial and marine SST signatures under certain insolation conditions. In addition, cause-and-effect drivers of past changes might also not be directly detected based on circulation-based climate regimes alone (or there might be significant temporal lags to drivers), and therefore a comprehensive approach of using proxy and models in tandem to reconstruct the past is certainly warranted for a region such as New Zealand.

## Conclusions

The main conclusions from this study are:

- The simulated temperatures of New Zealand for 6000 yr BP were lower compared with the pre-industrial control simulation.
- The lower temperatures were caused by an overall reduction in SSTs in the southwest Pacific in combination with lower insolation from December to June in the SH.
- The only season with relatively higher temperatures was SON, where the increase in SH insolation was at its peak.
- New Zealand was generally wetter in the 6000 yr BP simulations. However, the pattern of higher precipitation was restricted to northern and eastern areas of both islands from an anomalous easterly flow.
- The western South Island was drier as a result of the anomalous easterly flow in the 6000 yr BP simulations.
- Temperatures at 6000 yr BP were likely to be controlled more strongly by insolation and regional SSTs than by incident circulation, although the atmospheric circulation does have some influence.
- Proxy data suggest that the RCM output from the 6000 yr BP simulations are comparable with the period 7000–6000 yr BP for precipitation and atmospheric circulation.

These model simulations have demonstrated the usefulness of higher-resolution modelling using a Regional Climate Model, especially in a region such as New Zealand where the complex topography interacts strongly with the prevailing (westerly) atmospheric flow. However, this paper is only the first attempt at adequately modelling the climate of 6000 yr BP and further work should be undertaken to refine the method employed in this paper. In addition, refining the age controls on proxy archives, higher resolution proxies with more intensive sampling, quantitative reconstructions of climate, and additions to the proxy data base for New Zealand that cover the Holocene would greatly assist in the effort for undertaking meaningful proxy–model comparisons.

## Acknowledgements

This work contributes to the Adaptation to Climate Variability and Change programme (contracts C01X0202 and C01X0701), Modelling Palaeoclimate to Inform the Future programme (contract UOAX0213), and the Regional Climate Modelling to Develop Probabilistic Scenarios of Future New Zealand Climate (contract C01X0804) programme undertaken at NIWA (Wellington and Auckland). We acknowledge the international modeling groups for providing their SST data used in these simulations from the HadCM3\_UB and MIROC models and to the Laboratoire des Sciences du Climat et de l’Environnement (LSCE) for collecting and archiving those SST data.

## Funding

The PMIP2/MOTIF Data Archive is supported by CEA, CNRS, the EU project MOTIF (EVK2-CT-2002-00153) and the Programme National d'Etude de la Dynamique du Climat (PNEDC). The analyses were performed using version 04-02-2009 of the data base. More information is available on <http://pmip2.lsce.ipsl.fr/> and <http://motif.lsce.ipsl.fr/>.

## References

- Ackerley D, Dean S, Sood A et al. (2012) Regional climate modelling in New Zealand: Comparison to gridded and satellite observations. *Weather and Climate* 32(1): 3–22.
- Ackerley D, Lorrey A, Renwick JA et al. (2011a) Using synoptic type analysis to understand New Zealand climate during the mid-Holocene. *Climate of the Past* 7: 1189–1207.
- Ackerley D, Renwick JA, Huber M et al. (2011b) Modelling Eocene climate. *New Zealand Science Teacher* 127: 4–6,10.
- Anderson B and Mackintosh A (2006) Temperature change is the major driver of late-glacial and Holocene glacier fluctuations in New Zealand. *Geology* 34(2): 121–124, DOI: 10.1130/G22151.
- Braconnot P, Otto-Bliessner B, Harrison S et al. (2007a) Results of PMIP2 coupled simulations of the mid-Holocene and Last Glacial Maximum – Part 1: Experiments and large-scale features. *Climate of the Past* 3: 261–277.
- Braconnot P, Otto-Bliessner B, Harrison S et al. (2007b) Results of PMIP2 coupled simulations of the mid-Holocene and Last Glacial Maximum – Part 2: Feedbacks with emphasis on the location of the ITCZ and mid- and high latitudes heat budget. *Climate of the Past* 3: 279–296.
- Christensen JH, Kjellström E, Giorgi F et al. (2010) Weight assessment in regional climate models. *Climate Research* 44: 179–194.
- Drost F, Renwick J, Bhaskaran B et al. (2007) A simulation of New Zealand's climate during the Last Glacial Maximum. *Quaternary Science Reviews* 26: 2505–2525.
- Fletcher M-S and Moreno PI (2011) Have the Southern Westerlies changed in a zonally symmetric manner over the last 14,000 years? A hemisphere-wide take on a controversial problem. *Quaternary International* doi:10.1016/j.quaint.2011.04.042.
- Gómez-Navarro JJ, Montávez JP, Jerez S et al. (2011) A regional climate simulation over the Iberian Peninsula for the last millennium. *Climate of the Past* 7: 451–472.
- Gordon C, Cooper C, Senior CA et al. (2000) The simulation of SST, sea-ice extents and ocean heat transports in a version of the Hadley Centre Model without flux adjustments. *Climate Dynamics* 16: 147–168.
- Jones RG, Noguer M, Hassell DC et al. (2004) *Generating High Resolution Climate Change Scenarios Using PRECIS*. Exeter: Met Office Hadley Centre, 40 pp. Accessed 15 January 2012 from: <http://www.unclearn.org/sites/www.unclearn.org/files/inventory/UNDP17.pdf>
- K-1 Model Developers (2001) *K1 Coupled GCM (MIROC) Description*. Hasumi H and Emori S (eds) 34 pp. Accessed 8 November 2011 from: <http://www.ccsr.utokyo.ac.jp/kyosei/hasumi/MIROC/tech-repo.pdf>
- Kidson JW (2000) An analysis of New Zealand synoptic types and their use in defining weather regimes. *International Journal of Climatology* 20(3): 299–316.
- Kidston J, Renwick JA and McGregor J (2009) Hemispheric-scale seasonality in the Southern Annular Mode and impacts on the climate of New Zealand. *Journal of Climate* 22: 4759–4770.
- Koutavas A, Demenocal PB, Olive GC et al. (2006) Mid-Holocene El Niño–Southern Oscillation (ENSO) attenuation revealed by individual foraminifera in eastern tropical Pacific sediments. *Geology* 34(12): 993–996.
- Legutke S and Voss R (1999) *The Hamburg Atmosphere–Ocean Coupled Model ECHO-G*. Technical Report 18, German Climate Computer Center (DKRZ). Accessed 8 November 2011 from: <http://www.mad.zmaw.de/fileadmin/extern/documents/reports/ReportNo.18.pdf>
- Li X, Rapson GL and Flenley JR (2008) Holocene vegetational and climatic history, Sponge Swamp, Haast, south-western New Zealand. *Quaternary International* 184: 129–138.
- Lorrey AM, Fowler AM and Salinger J (2007) Regional climate regime classification as a qualitative tool for interpreting multi-proxy palaeoclimate data spatial patterns: A New Zealand case study. *Palaeogeography, Palaeoclimatology, Palaeoecology* 253: 407–433.
- Lorrey AM, Vandergoes M, Almond P et al. (2011) Palaeocirculation across New Zealand during the Last Glacial Maximum at ~21ka. *Quaternary Science Reviews* 36: 189–213, doi:10.1016/j.quascirev.2011.09.025.
- Lorrey AM, Vandergoes M, Renwick J et al. (2010) *A Regional Climate Regime Classification Synthesis for New Zealand Covering Three Critical Periods of the Late Quaternary: The Last 2000 Years, the Mid-Holocene, and the End of the Last Glacial Coldest Period*. NIWA Client Report AKL2010-025 prepared for the University of Auckland, 231 pp.
- Lorrey A, Williams P, Salinger J et al. (2008) Speleothem stable isotope records interpreted within a multi-proxy framework and implications for New Zealand palaeoclimate reconstruction. *Quaternary International* 187: 52–75.
- McGlone MS and Bathgate JL (1983) Vegetation and climate history of the Longwood Range, South Island, New Zealand. *New Zealand Journal of Botany* 21: 293–315.
- McGlone MS and Topping WW (1977) Arunian (post-glacial) pollen diagrams from the Tongariro region, North Island, New Zealand. *New Zealand Journal of Botany* 15: 749–760.
- McGlone MS, Salinger MJ and Moar NT (1993) Paleovegetation studies of New Zealand's climate since the Last Glacial Maximum. In: Wright HE Jr, Kutzbach JE, Webb T III et al. (eds) *Global Climates Since the Last Glacial Maximum*. Minneapolis: University of Minnesota Press, pp. 294–317.
- Martin TJ and Ogden J (2002) The seed ecology of *Ascarina lucida*: A rare New Zealand tree adapted to disturbance. *New Zealand Journal of Botany* 40: 397–404.
- Martin TJ and Ogden J (2005) Experimental studies on the drought, waterlogging, and frost tolerance of *Ascarina lucida* Hook. f. (Chloranthaceae) seedlings. *New Zealand Journal of Ecology* 29(1): 53–59.
- Moy CM, Seltzer GO, Rodbell DT et al. (2002) Variability of El Niño/Southern Oscillation activity at millennial timescales during the Holocene epoch. *Nature* 420: 162–165.
- Mullan AB (1998) Southern Hemisphere sea-surface temperatures and their contemporary and lag association with New Zealand temperature and precipitation. *International Journal of Climatology* 18: 817–840.
- Newnham RM, Lowe DJ and Green JD (1989) Palynology, vegetation, and climate of the Waikato lowlands, North Island, New Zealand, since c. 18,000 years ago. *Journal of the Royal Society of New Zealand* 19(2): 127–150.
- Ohgaito R and Abe-Ouchi A (2007) The role of ocean thermodynamics and dynamics in Asian summer monsoon changes during the mid-Holocene. *Climate Dynamics* 29: 39–50.
- Pfeiffer A and Zängl G (2011) Regional climate simulations for the European Alpine Region – Sensitivity of precipitation to large scale flow conditions of driving input data. *Theoretical and Applied Climatology* 105: 325–340, doi: 10.1007/s00704-010-0394-4.
- Phipps SJ, Rotstayn LD, Gordon HB et al. (2011) The CSIRO Mk3L climate system model version 1.0 – Part 1: Description and evaluation. *Geoscientific Model Development* 4: 483–509, doi:10.5194/gmd-4-483-2011.
- Phipps SJ, Rotstayn LD, Gordon HB et al. (2012) The CSIRO Mk3L climate system model version 1.0 – Part 2: Response to external forcings. *Geoscientific Model Development* 5: 649–682, doi:10.5194/gmd-5-649-2012.
- Pope VD, Gallani ML, Rowntree PR et al. (2000) The impact of new physical parametrizations in the Hadley Centre climate model: HadAM3. *Climate Dynamics* 16: 123–146.
- Renssen H, Goosse H, Fichefet T et al. (2005) Simulating the Holocene climate evolution at northern high latitudes using a coupled atmosphere–sea ice–ocean–vegetation model. *Climate Dynamics* 24: 23–43.
- Renwick JA (2011) Kidson's synoptic weather types and surface climate variability over New Zealand. *Weather and Climate* 31: 3–23.
- Rojas M and Moreno PI (2010) Atmospheric circulation changes and neoglacial conditions in the Southern Hemisphere mid-latitudes: Insights from PMIP2 simulations at 6 kyr. *Climate Dynamics* 37(1–2): 357–375.
- Rummukainen M (2010) State-of-the-art with regional climate models. *Climate Change* 1: 82–96.
- Salinger MJ (1980a) New Zealand climate I: Precipitation patterns. *Monthly Weather Review* 108: 1892–1904.
- Salinger MJ (1980b) New Zealand climate II: Temperature patterns. *Monthly Weather Review* 108: 1905–1912.
- Salinger MJ and Mullan AB (1999) New Zealand climate: Temperature and precipitation variations and their links with atmospheric circulation 1930–1994. *International Journal of Climatology* 19: 1049–1071.
- Schaefer JM, Denton GH, Kaplan M et al. (2009) High-frequency Holocene glacier fluctuations in New Zealand differ from the northern signature. *Science* 324: 622–625.
- Shulmeister J (1999) Australasian evidence for mid-Holocene climate change implies precessional control of the Walker Circulation in the Pacific. *Quaternary International* 57/58: 81–91.
- Singarayer JS and Valdes PJ (2010) High-latitude climate sensitivity to ice-sheet forcing over the last 120 kyr. *Quaternary Science Reviews* 29: 43–55.
- Strandberg G, Brandefelt J, Kjellström E et al. (2011) High resolution regional simulation of Last Glacial Maximum climate in Europe. *Tellus* 63A(1): 107–125.

- Tait A, Henderson R, Turner R et al. (2006) Thin plate smoothing spline interpolation of daily rainfall for NZ using a climatological rainfall scheme. *International Journal of Climatology* 26(14): 2097–2115, DOI:10.1002/joc.1350.
- Tait AB (2008) Future projections of growing degree days and frost in NZ and some implications for grape growing. *Weather and Climate* 28: 17–36.
- Thompson DWJ and Wallace JM (2000) Annular modes in the extratropical circulation. Part I: Month-to-month variability. *Journal of Climate* 13: 1000–1016.
- Vandergoes MJ, Newnham RM, Preusser F et al. (2005) Regional insolation forcing of late Quaternary climate change in the Southern Hemisphere. *Nature* 436: 242–245.
- Wagner S, Widmann M, Jones JM et al. (2007) Transient simulations, empirical reconstructions and forcing mechanisms for the mid-Holocene hydrological climate in southern Patagonia. *Climate Dynamics* 29: 333–355.
- Williams PW, Neil H and Zhao J-X (2010) Age frequency distribution and revised stable isotope curves for New Zealand speleothems: Paleoclimatic implications. *International Journal of Speleology* 39(2): 99–112.
- Zhang Q, Sundqvist HS, Moberg A et al. (2010) Climate change between the mid and late Holocene in northern high latitudes – Part 2: Model-data comparisons. *Climate of the Past* 6: 609–626.